Nitration Products of 5-Amino-1*H*-tetrazole and Methyl-5-amino-1*H*-tetrazoles – Structures and Properties of Promising Energetic Materials

by **Thomas M. Klapötke*** and **Jörg Stierstorfer**

Chair of Inorganic Chemistry, Energetic Materials Research, Ludwig-Maximilian University of Munich, Butenandtstrasse 5–13, D-81377 Munich
(phone: +4989218077491; fax: +4989218077492; e-mail: tmk@cup.uni-muenchen.de)

The nitration of 5-amino-1*H*-tetrazole (**1**), 5-amino-1-methyl-1*H*-tetrazole (**3**), and 5-amino-2-methyl-2*H*-tetrazole (**4**) with HNO_3 (100%) was undertaken, and the corresponding products 5-(nitrimino)-1*H*-tetrazole (**2**), 1-methyl-5-(nitrimino)-1*H*-tetrazole (**5**), and 2-methyl-5-(nitramino)-2*H*-tetrazole (**6**) were characterized comprehensively using vibrational (IR and *Raman*) spectroscopy, multinuclear (^1H, ^{13}C, ^{14}N, and ^{15}N) NMR spectroscopy, mass spectrometry, and elemental analysis. The molecular structures in the crystalline state were determined by single-crystal X-ray diffraction. The thermodynamic properties and thermal behavior were investigated by using differential scanning calorimetry (DSC), and the heats of formation were determined by bomb calorimetric measurements. Compounds **2**, **5**, and **6** were all found to be endothermic compounds. The thermal decompositions were investigated by gas-phase IR spectroscopy as well as DSC experiments. The heats of explosion, the detonation pressures, and velocities were calculated with the software EXPLO5, whereby the calculated values are similar to those of common explosives such as TNT and RDX. In addition, the sensitivities were tested by BAM methods (drophammer and friction) and correlated to the calculated electrostatic potentials. The explosion performance of **5** was investigated by *Koenen* steel sleeve test, whereby a higher explosion power compared to RDX was reached. Finally, the long-term stabilities at higher temperatures were tested by thermal safety calorimetry (FlexyTSC). X-Ray crystallography of monoclinic **2** and **6**, and orthorhombic **5** was performed.

1. Introduction. – The combination of a tetrazole ring with energetic groups containing oxygen such as nitro groups ($R-NO_2$) [1], nitrate esters ($R-O-NO_2$) [2], or nitramines (R_2N-NO_2) [3] is of particular interest. Energetic materials based on tetrazoles show the desirable properties of high N-atom contents on the one hand, and astonishing kinetic and thermal stabilities due to aromaticity on the other. Compounds with a high N-atom content are potential candidates for replacing common secondary explosives like RDX [4] (1,3,5-trinitro-1,3,5-triazinane) and HMX [5] (1,3,5,7-tetranitro-1,3,5,7-tetrazocane), or for use in high-tech propellants when combined with a suitable oxidizer [6]. Nitraminotetrazoles are of special interest because they combine both the oxidizer and energetic N-rich backbone in one molecule.

The nomenclature of 5-(nitroamino)tetrazoles, also referred to as (nitramino)- or (nitrimino)tetrazoles, is usually inconsistent in literature [7], as a result of incomplete characterization of the previously reported compounds. Therefore, a complete characterization of three well-known (nitro-amino)tetrazoles is given in this work. The crystal structures show the first examples of neutral 5-amino-1*H*-tetrazoles which

have been nitrated at the primary NH_2 group. For 5-(nitrimino)tetrazole, only the cell parameters have been previously published [8], while several examples of *N*-methyl-*N*-nitro-5-amino-1*H*-tetrazoles have been structurally characterized and reported in the literature [9]. On the basis of the crystal structures obtained, the nitration product of 5-amino-1*H*-tetrazole (5-AT; **1**) is now referred to as 4,5-dihydro-5-(nitrimino)-1*H*-tetrazole (**2**; *cf. Scheme* below).

(Nitrimino)tetrazoles and corresponding metal (nitramino)tetrazolates [10–12] have been known for a long time, since they are cheap and easy to manufacture *via* various routes. However, there are two main methods. The first synthesis involves protonation of 5-amino-1*H*-tetrazole (5-AT, **1**) [13] using warm concentrated HNO_3, to form 5-amino-1*H*-tetrazolium nitrate [14], followed by dehydration with concentrated H_2SO_4 [15] to form **2**. Another synthetic route is based on the cyclization of nitroguanyl azide [16][17] (also known as (nitroazido)formamidine). A further method is the *N*-nitration of aminotetrazoles using tetranitromethane [18].

2. Results and Discussion. – 2.1. *Synthesis.* The syntheses of 4,5-dihydro-5-(nitrimino)-1*H*-tetrazole (**2**), 4,5-dihydro-1-methyl-5-(nitrimino)-1*H*-tetrazole (**5**), and 2-methyl-5-(nitramino)-2*H*-tetrazole (**6**) are presented in the *Scheme*. All of the syntheses are facile one-pot reactions using 100% HNO_3, whereby the products are available by evaporation of the solvent in high quantities and good yields. Single crystals of **2**, **5**, and **6** can be obtained by recrystallization from EtOH. Recrystallization of **2** and **5** from H_2O yield the monohydrates, not described in this work.

Scheme. *The Reactions of 5-Amino-1*H*-tetrazole* (**1**; 5-AT), *1-Methyl-5-amino-1*H*-tetrazole* (**3**), *and 2-Methyl-5-amino-2*H*-tetrazole* (**4**) *with 100% HNO_3*

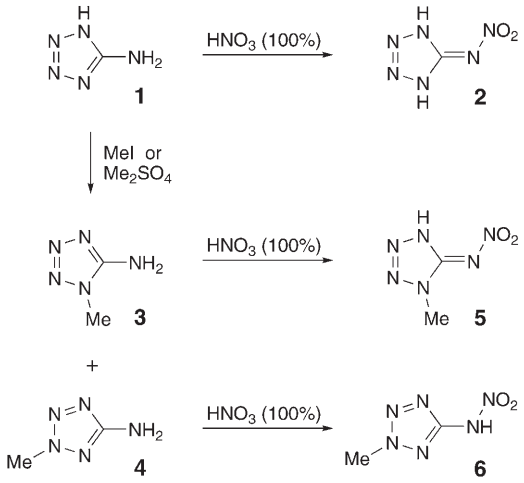

2.2. *Molecular Structures.* The single-crystal X-ray diffraction data were collected using an *Oxford Xcalibur3* diffractometer with a *Spellman* generator (voltage 50 kV, current 40 mA) and a *Kappa CCD* detector. The data collections were undertaken using the CrysAlis CCD software [19], and the data reductions were performed with the CrysAlis RED software [20]. The structures were solved with SIR-92 [21] and

refined with SHELXL-97 [22], and finally checked using PLATON [23]. In all structures, the H-atoms were located and refined. The absorptions of **5** and **6** were corrected using the SCALE3 ABSPACK multi-scan method [24]. In the chiral space group $P2_12_12_1$, the *Friedel* pairs were merged. Selected data from the X-ray data collection and refinements are given in *Table 1*[1]).

Table 1. *Crystallographic Data of* **2**–**6**

	2	**5**	**6**
Formula	$CH_2N_6O_2$	$C_2H_4N_6O_2$	$C_2H_4N_6O_2$
Form. weight [g mol^{-1}]	130.09	144.11	144.11
Crystal system	Monoclinic	Orthorhombic	Monoclinic
Space Group	$P2_1/c$ (14)	$P2_12_12_1$ (19)	$P2_1/c$ (14)
Color/habit	colorless cuboids	colorless rods	colorless blocks
Size [mm]	$0.18 \times 0.13 \times 0.08$	$0.19 \times 0.16 \times 0.08$	$0.24 \times 0.18 \times 0.15$
a [Å]	9.4010(3)	6.6140(1)	9.5278(9)
b [Å]	5.4918(1)	8.5672(2)	7.7308(7)
c [Å]	9.3150(3)	19.2473(4)	8.4598(9)
α [°]	90.0	90.0	90.0
β [°]	105.762(3)	90.0	112.875(9)
γ [°]	90.0	90.0	90
V [Å^3]	462.84(2)	1090.62(4)	574.1(1)
Z	4	8	4
$\rho_{calc.}$ [g cm^{-3}]	1.867	1.755	1.667
μ [mm^{-1}]	0.169	0.153	0.145
$F(000)$	264	592	296
$\lambda(MoK_\alpha)$, [Å]	0.71073	0.71073	0.71073
T [K]	100	100	200
θ (min, max) [°]	4.3, 32.1	3.7, 32.1	4.6, 26.0
Dataset	−13: 13; −8: 8; −13: 13	−9: 9; −12: 12; −28: 27	−11: 11; −9: 9; −10: 10
Reflections collected	6375	15881	5625
Independent reflections	1537	2104	1128
R_{int}	0.037	0.034	0.034
Observed reflections	1050	1616	1087
parameters	90	213	107
R_1 (obs.)	0.0343	0.0297	0.0440
wR_2 (all data)	0.0960	0.0696	0.0950
Goodness-of-fit	1.00	0.99	1.21
Weighting scheme	0.05710	0.04220	0.03930, 0.16880
Resd. dens. [e/Å^3]	−0.23, 0.31	−0.32, 0.21	−0.22, 0.17
Device type	*Oxford Xcalibur3 CCD*	*Oxford Xcalibur3 CCD*	*Oxford Xcalibur3 CCD*
Solution	SIR-92	SIR-92	SIR-92
Refinement	SHELXL97	SHELXL97	SHELXL97
Absorption correction	none	multi-scan	multi-scan
CCDC No.	635164	635163	635160

[1]) Further information regarding the crystal-structure determinations has been deposited with the *Cambridge Crystallographic Data Centre* as supplementary publication No. 635164 (**2**), 635163 (**5**) and 635160 (**6**).

Compound **2** was characterized as a dibasic acid with pK_a values of 2.5 and 6.1 [15]; previously it was not possible to locate the H-atoms, and it was assumed that the more acidic H-atom is located at the nitramino group [25]. However, using single crystal-diffraction both H-atoms were located on the tetrazole ring at N(1) and N(4). The ^{15}N-NMR spectra (see below) shows only four signals, which suggests the same connectivity present in solution. Even in the gas phase, DFT calculations (see below) indicate this isomer as being lowest in energy. The molecular unit can be seen in *Fig. 1*.

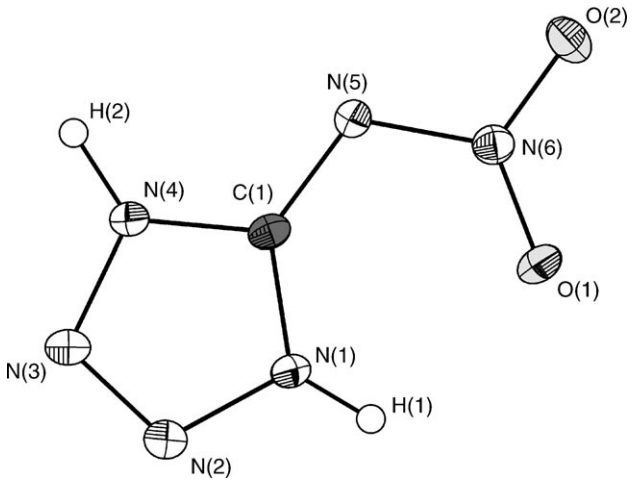

Fig. 1. *A view of the molecular structure of* **2** (thermal ellipsoids at 50% probability level, H-atoms shown as small spheres of arbitrary radii)

The geometry of the tetrazole ring in **2** can be compared with that of 5-amino-1*H*-tetrazole monohydrate (5-AT, **1**) [26]. The bond lengths in **2** are by *ca.* 1 Å shorter than in **1**, with the shortest distance in **2** between the atoms N(2) and N(3) with 1.278(1) Å and the longest between N(1) and N(2) with 1.358(1) Å. The C(1)–N(5) bond length is 1.341(1) Å, which is closer to a C,N double bond (1.28 Å) rather than to a C,N single bond (1.46 Å), whereas the nitramine bond N(5)–N(6) is considerably longer (1.363(1) Å). The angles in **2** differ in comparison with those in **1**. The N(4)–C(1)–N(1) angle in **2** (103.9(1)°) is smaller than that in **1** (107.9(1)°), which can be explained using the VSEPR model [27], in which a double bond requires more space. A condition of the 6π-*Hückel* aromaticity is a planar ring system, which can be seen at the torsion angle N(1)–N(2)–N(3)–N(4) of 0.5(1)°. The nitramine group also shows only slight derivations from the planarity (torsion angle C(1)–N(5)–N(6)–O(1) 1.8(1)°), and is stabilized *via* an intramolecular H-bond between N(1)–H(1)–O(1). In addition, there are several intermolecular H-bonds illustrated in *Fig. 2*, which are one reason for the high density of 1.867 g/cm^3. The strongest intermolecular H-bonds are between N(1) and N(2)^i d(D–H) 2.948(1) Å, $\angle$(D–H–A) 156(1)°, *i:* $1-x, 0.5+y, 1.5-z$) and the atoms N(4) and N(5)^{ii} d(D–A) 2.850(2) Å, $\angle$(D–H–A) 175(2)°, *ii:* $2-x, -0.5+y, 1.5-z$). Bond lengths and angles for the non-H-atoms in **2** are given in *Tables 2* and *3*.

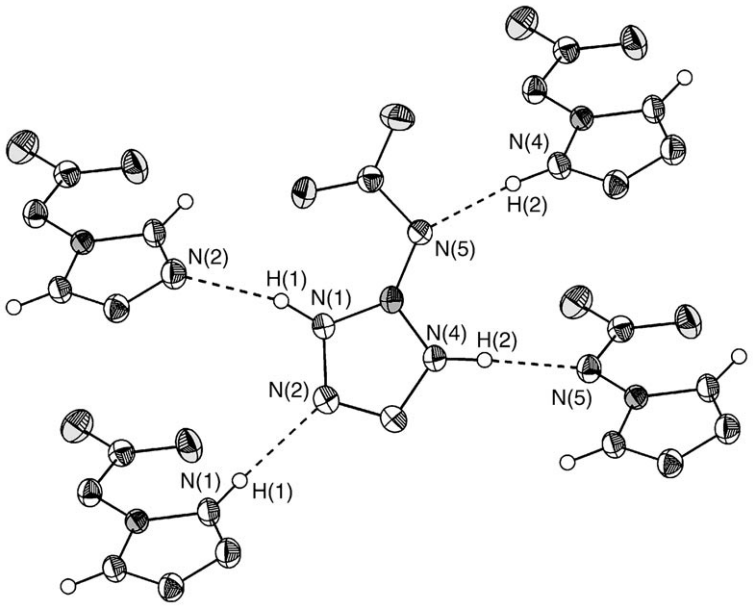

Fig. 2. *H-Bonding in* **2**. N(1)–H(1)–N(2)^{i}: *d*(D–H) 0.89(2) Å, *d*(H–A) 2.11(2) Å, *d*(D–A) 2.948(1) Å, ∠(D–H–A) 156(1)°; N(4)–H(2)–N(5)^{ii}: 0.98(2) Å, 1.83(2) Å, 2.850(2) Å, 175(2)°; N(4)–H(2)–O(2)^{ii}: 0.98(2) Å, 2.48(2) Å, 3.146(1) Å, 125(1)°; N(4)–H(2)–N(6)^{ii}: 0.98(2) Å, 2.58(2) Å, 3.4748(14) Å, 153(1)°; *i*: $1-x$, $0.5+y$, $1.5-z$; *ii*: $2-x$, $-0.5+y$, $1.5-z$.

Table 2. *Bond Lengths* d [Å] *of* **2**, **5**, *and* **6**

	2	**5**	**6**
O(2)–N(6)	1.234(1)	1.234(2)	1.224(2)
O(1)–N(6)	1.237(1)	1.266(2)	1.217(2)
N(1)–N(2)	1.358(1)	1.355(2)	1.327(2)
N(1)–C(1)	1.341(1)	1.345(2)	1.325(2)
N(4)–C(1)	1.336(1)	1.338(2)	1.339(2)
N(4)–N(3)	1.352(1)	1.364(2)	1.321(2)
N(2)–N(3)	1.278(1)	1.284(2)	1.318(2)
N(5)–N(6)	1.363(1)	1.338(2)	1.379(2)
N(5)–C(1)	1.341(1)	1.346(2)	1.397(2)
N(1,2)–C(2)		1.455(2)	1.459(2)

Accordingly, the densities of **5** and **6** decrease because of the presence of a Me group. The molecular unit of **5** (*Fig. 3*) shows a similar connectivity to that of **2**, whereby the H-atom at N(1) in **2** has been substituted by a Me group. Again, in **5** the NO_2 group is tilted to the side where the H-atom is located, forming an intramolecular H-bond. In **5**, the nitrimine unit is also found to lie in the plane of the tetrazole ring (torsion angle O(1)–N(6)–N(5)–C(1) of 4.3(2)°), whereby the tetrazole ring in **5** shows comparable bond lengths with those observed in **2**. The most significant difference is the nitramine bond between N(5) and N(6), which is shorter in compound

Table 3. *Bond Angles* [°] *of* **2**, **5**, *and* **6**

	2	**5**	**6**
N(2)–N(1)–C(1)	109.87(9)	110.4(1)	101.0(1)
C(1)–N(4)–N(3)	110.5(1)	110.2(1)	105.8(1)
N(1)–N(2)–N(3)	107.97(9)	107.8(1)	114.1(1)
N(6)–N(5)–C(1)	115.43(9)	11567(1)	117.9(1)
N(2)–N(3)–N(4)	107.73(9)	107.7(1)	106.0(1)
N(1)–N(2)–C(2)		122.0(1)	
C(1)–N(1)–C(2)		127.3(1)	
N(2)–N(3)–C(2)			122.1(1)
N(1)–N(2)–C(2)			123.8(1)
O(1)–N(6)–O(2)	123.5(1)	121.6(1)	126.1(2)
O(1)–N(6)–N(5)	122.07(9)	121.9(1)	118.2(1)
O(2)–N(6)–N(5)	114.44(9)	116.5(1)	115.6(2)
N(4)–C(1)–N(1)	103.9(1)	103.9(1)	113.2(2)
N(4)–C(1)–N(5)	121.4(1)	136.9(1)	122.3(1)
N(1)–C(1)–N(5)	134.6(1)	119.2(1)	124.5(2)

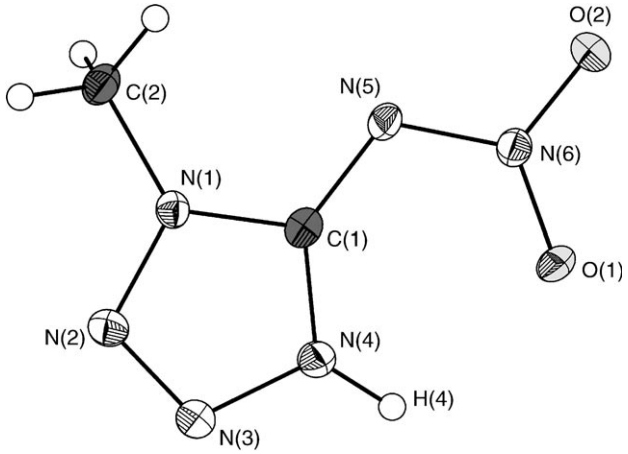

Fig. 3. *A view of the molecular structure of* **5**, *representing the half of the asymmetric unit* (thermal ellipsoids at 50% probability level, H-atoms shown as small spheres of arbitrary radii)

5 (d(N(5)–N(6)) 1.338(2) Å). Finally, there are no significant differences for the angles observed in compound **2** and **5**.

The structure observed for **5** in the crystalline state is again influenced by several strong intermolecular H-bonds, which are illustrated in *Fig. 4*.

The structure of **6** is considerably different from the structures of **2** and **5** discussed above. The Me group at N(2) directs the remaining H-atom to N(5), building a nitraminotetrazole (*Fig. 5*). In **6**, the C(1)–N(5) bond length (1.337(2) Å) is crucially longer, and the nitramine unit does not lie in the plane of the tetrazole ring, as is clearly shown by the C(1)–N(5)–N(6)–O(1) torsion angle of –19.2(2)°. The N(6)–N(5)–C(1) angle (117.9(1)°) is larger than observed in **2** and **5**, and the

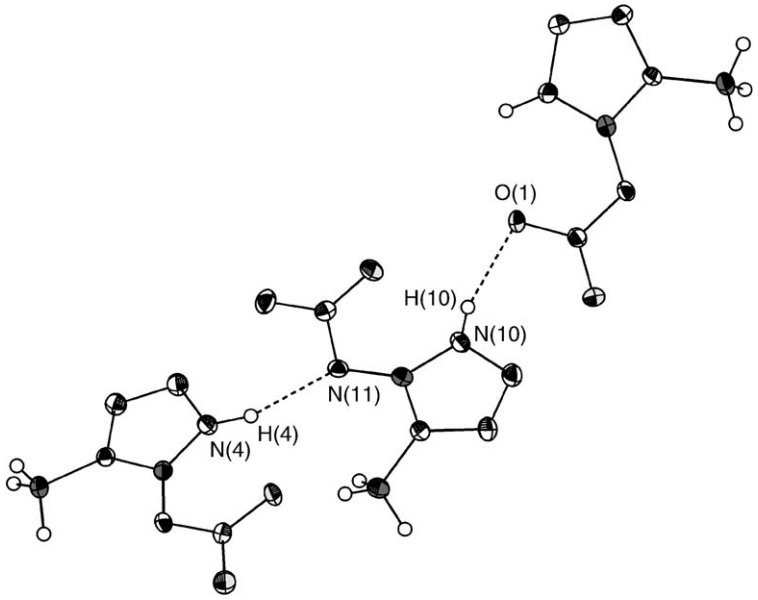

Fig. 4. *H-Bonding in* **5**. N(4)–H(4)–N(11)^{i}: d(D–H) 0.93(2) Å, d(H–A) 1.96(2) Å, d(D–A) 2.848(2) Å, ∠(D–H–A) 158(2)°; N(4)–H(4)–O(4)^{i}: 0.93(19) Å, 2.59(2) Å, 3.098(2) Å, 115.3(15)°; N(10)–H(10)–O(1)^{i}: 0.80(2) Å, 2.10(2) Å, 2.874(2) Å, 163(2)°; i: $-x$, $0.5+y$, $0.5-z$.

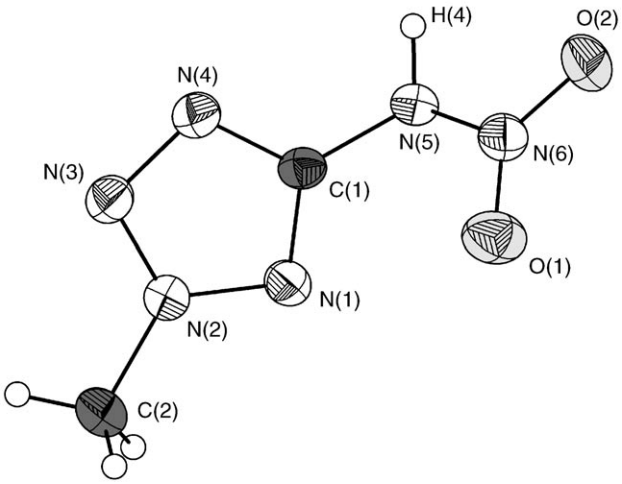

Fig. 5. *A view of the molecular structure of* **6** (thermal ellipsoids drawn at 50% probability level)

N(5)–N(6) nitramine bond of 1.379(2) Å is the longest in this series of compounds, which can be seen as contributing to the low density of 1.667 g/cm^3, which is the lowest among the three structures discussed in this work. Further reasons for the lower observed density of **6** are the absence of strong intramolecular H-bonds and the

presence of only two moderately strong H-bonds as are illustrated in *Fig. 6*. Relevant structural parameters are listed below.

2.3. *Spectroscopy.* 2.3.1. *Vibrational Spectroscopy.* Vibrational spectroscopy is a suitable method for identifying (nitramino)tetrazoles. The IR and *Raman* (*Fig. 7*)

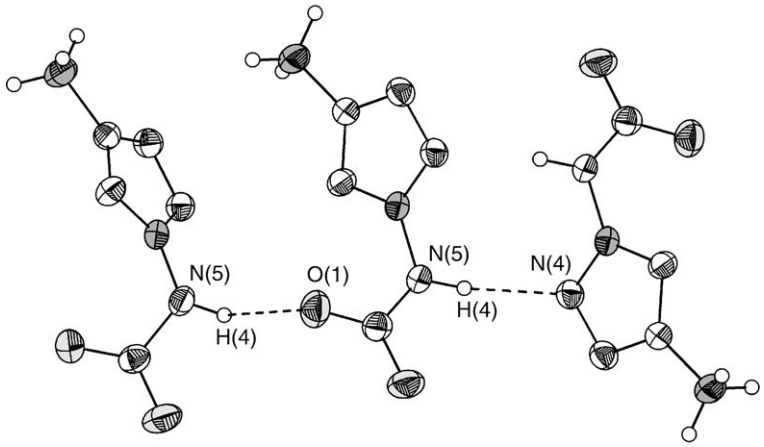

Fig. 6. *H-Bonding in* **6**. N(5)–H(4)–N(4)^{i}: *d*(D–H) 0.86(2) Å, *d*(H–A) 2.13(2) Å, *d*(D–A) 2.965(2) Å, ∠(D–H–A) 163(2)°; N(5)–H(4)–O(1)^{ii}: 0.86(2) Å, 2.66(2) Å, 3.070(2) Å, 111(2)°; *i*: $-x, -y, 2-z$; *ii*: $x, 0.5-y, 0.5+z$.

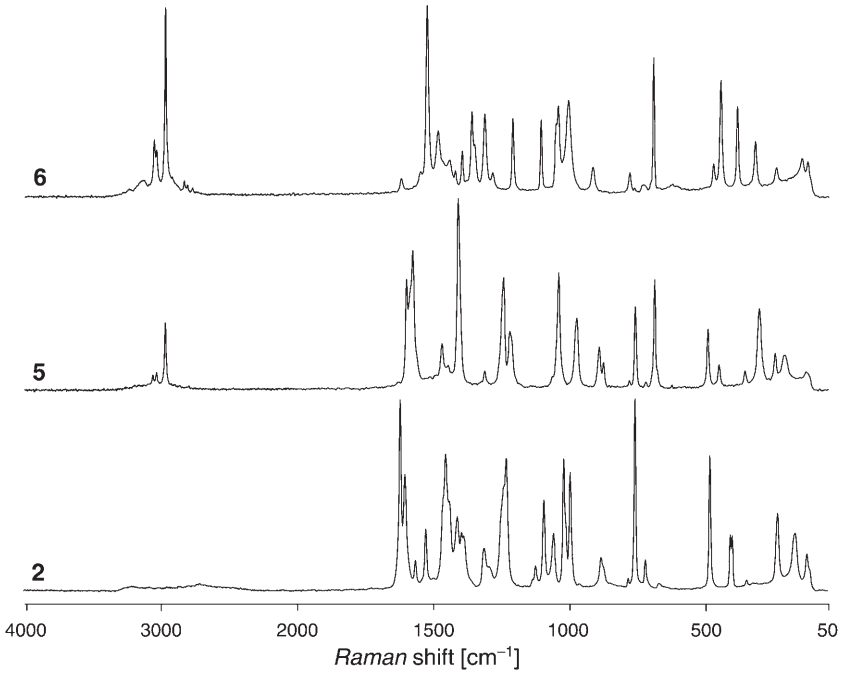

Fig. 7. *Solid-state* Raman *spectra of compounds* **2**, **5**, *and* **6**

spectra of compounds **2**, **5**, and **6** show the vibrations expected from comparison with spectra of similar compounds in the literature [28][29]. The $N-NO_2$ groups result in strong absorptions in the 1280–1300 ($\tilde{\nu}_{sym}(NO_2)$) and 1560–1620 ($\tilde{\nu}_{asym}(NO_2)$) cm^{-1} regions as well as in a weak band at 945–970 ($\nu(N-N)$) cm^{-1} [30]. The IR and *Raman* spectra of compounds **2**, **5**, and **6** show further characteristic absorption bands in regions as follows: 3250–3100 cm^{-1} ($\tilde{\nu}(N-H)$), 3000–2850 ($\tilde{\nu}(C-H)$ **5** and **6**), 1680–1550 ($\tilde{\nu}(N-H)$), 1550–1350 ($\tilde{\nu}$, tetrazole ring, $\tilde{\nu}_{as}(Me)$), *ca.* 1380 ($\tilde{\nu}(Me)$), 1350–700 ($\tilde{\nu}(N(1)-C(1)-N(4))$, $\tilde{\nu}(N-N)$, $\tilde{\nu}(N-H)$, $\tilde{\nu}$, tetrazole ring), <700 ($\nu\ \delta_{oop}\ N-H$)).

2.3.2. *NMR Spectroscopy.* The ^{13}C- and ^{15}N-NMR chemical shifts and the $^{15}N,^{1}H$ coupling constants are presented in *Table 4* and can be seen in *Fig. 8*. For all compounds, the H-coupled as well as the H-decoupled ^{15}N-NMR spectra (with full NOE) were recorded. The assignments are given based on the values of the $^{15}N,^{1}H$ coupling constants and on comparison with the literature [9]. The chemical shifts are given with respect to $MeNO_2$ (^{15}N) and TMS (^{13}C) as external standards. In the case of ^{15}N-NMR, negative shifts are upfield from $MeNO_2$. For all compounds, (D_6)DMSO

Table 4. *^{15}N- and ^{13}C-NMR Chemical Shifts* δ [ppm] *and $^{15}N,^{1}H$-Coupling Constants* J [Hz] *of* **2**, **5**, *and* **6**

	2		**5**	**6**
	((D_6)Acetone)	((D_6)DMSO)	((D_6)DMSO)	((D_6)DMSO)
N(1)	– 143.4	– 144.6	– 177.4 (^{2}J(N,H) = 2.1)	– 83.4 (^{3}J(N,H) = 1.9)
N(2)	– 26.4	– 24.6	– 26.8 (^{3}J(N,H) = 1.9)	– 103.6 (^{2}J(N,H) = 2.2)
N(3)	– 26.4	– 24.6	– 29.8	– 0.3 (^{3}J(N,H) = 1.9)
N(4)	– 143.4	– 144.6	– 159.2	– 58.3
N(5)	– 143.3	– 174.9	– 159.3	– 209.3
N(6)	– 29	– 24.6	– 18.8	– 35
C(1)	151.8	152.6	150.3	157.6

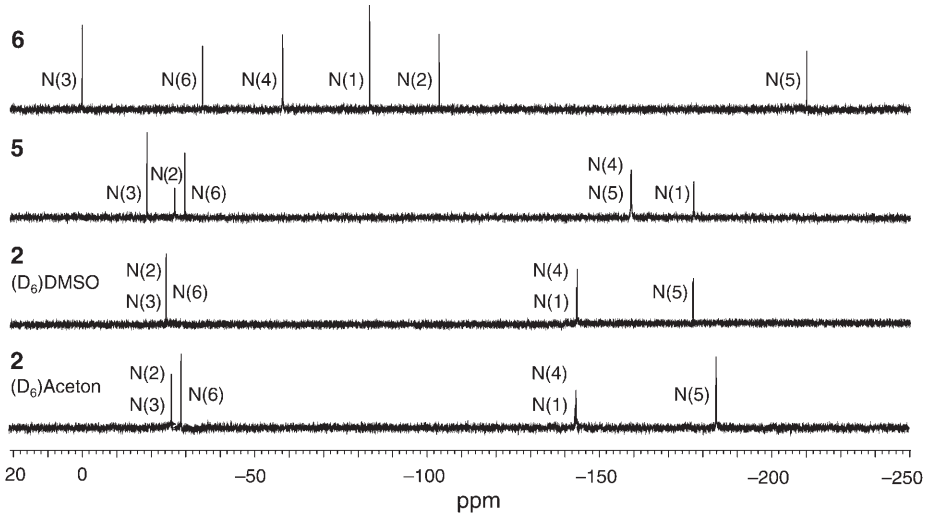

Fig. 8. *^{15}N-NMR Spectra of compounds* **2**, **5**, *and* **6**

was used as the solvent, and (D_6)acetone was used for observing the solvent shift in compound **2**. In the (D_6)DMSO spectra, only three signals could be observed for **2**, while in (D_6)acetone the five expected signals could be located and assigned.

2.4. *Thermodynamic and Energetic Properties.* 2.4.1. *Differential Scanning Calorimetry* (*DSC*). DSC Measurements to determine the decomposition temperatures of **2**, **5**, and **6** were performed in covered Al containers with a N_2 flow of 20 ml/min on a *Perkin-Elmer Pyris 6 DSC* [31], calibrated by standard pure In and Zn at a heating rate of 5°/min. The DSC plots in *Fig. 9* show the thermal behavior of 1.0 mg of **2**, **5** and **6** in the temperature range of 50–300°. Compound **2** shows the lowest decomposition point at 122°, whereby compounds **5** and **6** decompose during melting at 125° and 123°, as is shown by the curve of *Fig. 9*.

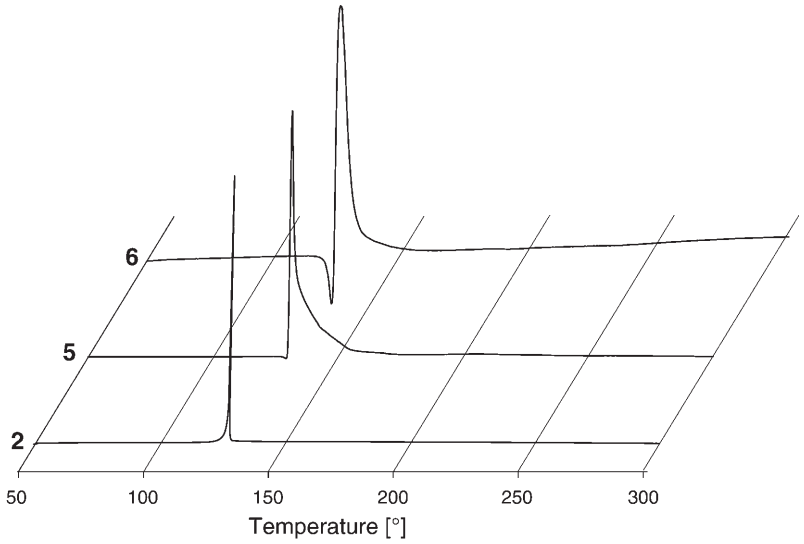

Fig. 9. *DSC Plot* (endo up) *of compounds* **2**, **5**, *and* **6** (5°/min; T_{onset} **2**: 122°, **5**: 125°, **6** 123°)

To determine the heats of decomposition, a *Linseis DSC PT10* [32] was used. Three samples (*ca.* 1 mg) were heated with a heating rate of 2°/min and a fixed N_2 flow of 5 l/h over the decomposition peaks. The surface was integrated using the Linseis software, and the average of three measurements was calculated to yield heats of decomposition ΔH^0_{dec} of 2638 J/g (**2**), 1685 J/g (**5**), and 2158 J/g (**6**).

2.4.2. *Bomb Calorimetry.* The heats of combustion for the compounds **2**, **5**, and **6** were determined experimentally, using a *Parr 1356* bomb calorimeter (static jacket) equipped with a *Parr 1108CL* O_2 bomb [33]. To ensure better combustion, the samples (*ca.* 200 mg) were pressed with a defined amount of benzoic acid (*ca.* 800 mg) forming a tablet, and a *Parr 45C10* alloy fuse wire was used for ignition. In all measurements, a correction of 2.3 cal/cm wire burned has been applied, and the bomb was examined for evidence of noncombusted carbon after each run. A *Parr 1755* printer was furnished with the *Parr 1356* calorimeter to produce a permanent record of all activities within the calorimeter. The reported values are the average of three separate measurements. The calorimeter was calibrated by combustion of certified benzoic acid (SRM, 39i, NIST) in

an O_2 atmosphere at a pressure of 3.05 mPa. The experimental results of the constant-volume combustion energy (ΔU_c) of the salts are summarized in *Table 5*. The standard molar enthalpy of combustion (ΔH_c^0) was derived from $\Delta H_c^0 = \Delta U_c + \Delta nRT$ ($\Delta n = \Delta n_i$ (products, g) – Δn_i(reactants, g); Δn_i is the total molar amount of gases in the products or reactants). The enthalpy of formation, ΔH_f^0 for each of the compounds was calculated at 298.15 K using *Hess*' law and the following combustion reactions (*Eqns. 1* and *2*), which show that **2**, **5**, and **6** are strongly endothermic compounds (ΔH_f^0: **2**: + 264 kJ/mol, **5**: + 260 kJ/mol, **6**: + 380 kJ/mol).

$$CH_2N_6O_2\ (\mathbf{2}) + ½\ O_2 \rightarrow CO_2 + H_2O + 3\ N_2 \quad (1)$$

$$C_2H_4N_6O_2\ (\mathbf{5}, \mathbf{6}) + 2\ O_2 \rightarrow 2\ CO_2 + 2\ H_2O + 3\ N_2 \quad (2)$$

Table 5. *Physico-Chemical Properties of* **2**, **5**, *and* **6**

	2	**5**	**6**
Formula	$CH_2N_6O_2$	$C_2H_4N_6O_2$	$C_2H_4N_6O_2$
Molecular Mass [g/mol]	130.09	144.11	144.11
Impact sensitivity [J][a])	1.5	12.5	3.0
Friction sensitivity [N][b])	8	160	145
Electrical discharge	no reaction	no reaction	no reaction
N [%][c])	64.61	58.32	58.32
Ω [%][d])	− 12.30	− 44.41	− 44.41
Combustion	yes	yes	yes
$T_{dec.}$ [°][e])	122	125	122
Density [g/cm^3][f])	1.87	1.76	1.67
$-\Delta U_c$ [cal/g][g])	1750	2700	2902
$-\Delta H_c$ [kJ/mol][h])	944	1619	1740
ΔH_{fm}^0 [kJ/mol][i])	264	260	380
ΔH_{decm}^0 [J/g][j])	2638	1685	2158
$-\Delta U_{Em}^0$ [J/g][k])	5326	5235	5998
T_E [K][l])	4309	3824	4283
p [kbar][m])	363	295	289
D [m/s][n])	9173	8433	8434
Gas vol. [ml g^{-1}][o])	404	395	413

[a])[b]) BAM Methods, see [34][35][2]). [c]) Nitrogen content. [d]) Oxygen balance. [e]) Decomposition temperature from DSC (5° min^{-1}). [f]) Estimated from X-ray diffraction. [g]) Experimental (constant volume) combustion energy. [h]) Experimental molar enthalpy of combustion. [i]) Molar enthalpy of formation. [j]) Experimental enthalpy of decomposition using DSC. [k]) Energy of explosion, EXPLO5 V5.02. [l]) Explosion temperature, EXPLO5 V5.02. [m]) Detonation pressure, EXPLO5 V5.02. [n]) Detonation velocity, EXPLO5 V5.02. [o]) Assuming only gaseous products, EXPLO5 V5.02.

The enthalpies of energetic materials are governed by the molecular structure of the compounds, and, therefore, heterocycles with a higher N content (*e.g.*, imidazole

[2]) Impact: insensitive > 40 J, less sensitive ≥ 35 J, sensitive ≥ 4, very sensitive ≤ 3 J; friction: insensitive > 360 N, less sensitive = 360 N, sensitive < 360 N and > 80 N, very sensitive ≤ 80 N, extreme sensitive ≤ 10 N; according to the *UN Recommendations on the Transport of Dangerous Goods* [36] (+) indicates: not safe for transport.

($\Delta H^0_{f\,cryst} = 14.0$ kcal/mol) [34]; 1,2,4-triazole ($\Delta H^0_{f\,cryst} = 26.1$ kcal/mol); ($\Delta H^0_{f\,cryst} = 56.7$ kcal/mol)) [35] show higher heats of formation. From the experimentally determined heats of formation and densities obtained from single-crystal structure X-ray diffraction, various thermochemical properties have been calculated using the EXPLO5 software (see below) and are summarized in *Table 5*.

2.4.3. *Sensitivities.* For initial safety testing, the impact and friction sensitivities were tested according to BAM methods[2]) [37] with the 'BAM Fallhammer' and 'BAM friction tester'. Compound **2** is very sensitive towards impact (< 1.5 J) and friction (< 8 N), and, since the value is comparable with lead azide, it should be considered to be a primary explosive and should, therefore, only be handled with appropriate precautions. Compound **5** is moderately sensitive towards impact (< 12.5 J) and friction (< 160 N), however, **6** shows increased sensitivities (impact: < 3.0 J, friction: < 145 N). Accordingly, **5** and **6** fall into the group of compounds described as 'sensitive'.

2.4.4. *Decomposition Products.* To determine the thermal decomposition [38] products, the compounds were heated in an evacuated steel tube for *ca.* 30 s about 100° above the decomposition temperature, and the gaseous products were transferred into an evacuated gas IR cell. In *Fig. 10*, the gas-phase IR spectra of the decomposition products of **2**, **5**, and **6** are shown.

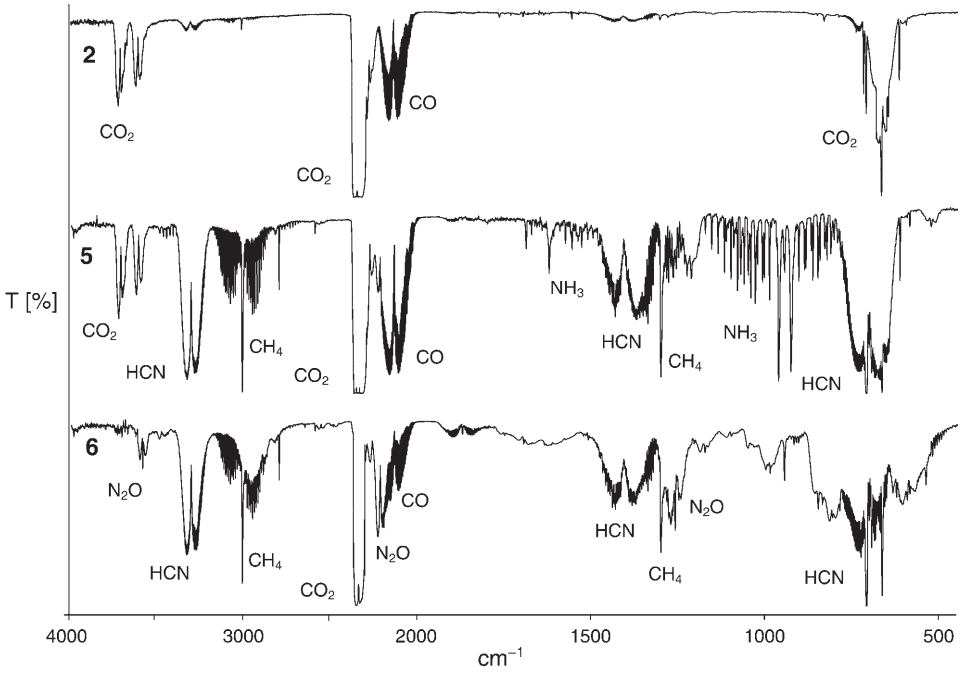

Fig. 10. *IR Spectra showing the gas-phase decomposition products of* **2**, **5**, *and* **6**

The thermal decomposition of **2** results in the formation of only two main products which could be identified using IR spectroscopy, namely CO_2 [39] and CO [40]. In

addition, trace amounts of HCN and CH_4 were visible in the gas-phase IR spectrum; however, no evidence for the formation of water vapor was found. In the methylated compounds, many more decomposition products were observed using gas-phase IR spectroscopy. Besides CO_2 and CO, larger amounts of CH_4 [41] and HCN were found in the decomposition of **5** and **6**, in comparison with **2**. In contrary to **5**, where bigger amounts of expected NH_3 were detected, the thermal decomposition of **6** shows only traces of NH_3 but moderate amounts of N_2O [42].

2.4.5. *Detonation Parameter.* The detonation parameters were calculated with the program EXPLO5 V5.02 [43]. The program is based on the steady-state model of equilibrium detonation and uses BKW E.O.S. for gaseous detonation products and *Cowan-Fickett* E.O.S. for solid carbon. The calculations were performed using the maximum densities according to the crystal structures, and the BKWN set of constants was used. Compound **2** shows a very high calculated detonation pressure of 363 kbar and a detonation velocity of 9173 m/s higher than TNT ($p = 202$ kbar, $v = 7150$ m/s). Even compound **5** also shows promising values for the detonation pressures (295 kbar) and explosion velocity (8433 m/s). The influence of the density on the properties of energetic materials is clearly shown by **6**, which shows the lowest detonation pressure of 289 kbar in spite of the highest positive heat of formation due to its low density.

2.4.6. Koenen *Test.* The explosion performance under confinement of compound **5** was investigated using a '*Koenen* test' steel sleeve apparatus [34][35]. Data obtained from the *Koenen* test can be related to the performance of the compound and can be used to determine the shipping classification of a substance, and for evaluating the degree of venting required to avoid an explosion during processing operations. This test uses a non-reusable open-ended flanged steel tube, a closing device with a variable orifice (0–10 mm), through which gases formed on decomposition are vented, industrial propane cylinder, and four *Bunsen* burners. For the test, a defined volume of 25 ml of the compound is loaded into a flanged steel tube, and a threaded collar is slipped onto the tube from below. The closing plate with the orifice is fitted over the flanged tube and secured with a nut. Heating is provided by four propane burners that are ignited simultaneously. The test is completed when either rupture of the tube is observed, or, no reaction is observed, after heating the tube for a minimum of 5 min. After each trial, the fragments of the tube, if any, are collected and weighed. The reaction is evaluated as an explosion if the tube is fragmented into three or more pieces. TNT (Trinitrotoluol) destroys the steel tube up to a hole width of 6 mm, RDX (Royal Demolition Explosive) achieves this even with a hole width of 8 mm. The result of the *Koenen* test can be seen in *Fig. 11*. Compound **5** destroyed the steel tube into more than 20 fragments using a hole width of 8 mm as well with a hole of 10 mm, and it can, therefore, be assumed that compound **5** offers a greater explosion performance compared to RDX.

2.4.7. *Long-Term Stability Tests.* Long term stability tests were performed using a *Systag FlexyTSC* [44] (thermal safety calorimetry) in combination with a *RADEX V5* oven and the SysGraph Software. The tests were conducted as long-term isoperibolic evaluations in *Glass* test vessels at atmospheric pressure with *ca.* 300 mg of the compounds. It was shown that tempering the substance for 48 h at 40° under the decomposition point results in a storage period of 58 years at room temperature. In our cases, we chose a temperature of 80° and investigated the possible occurrence of exo-

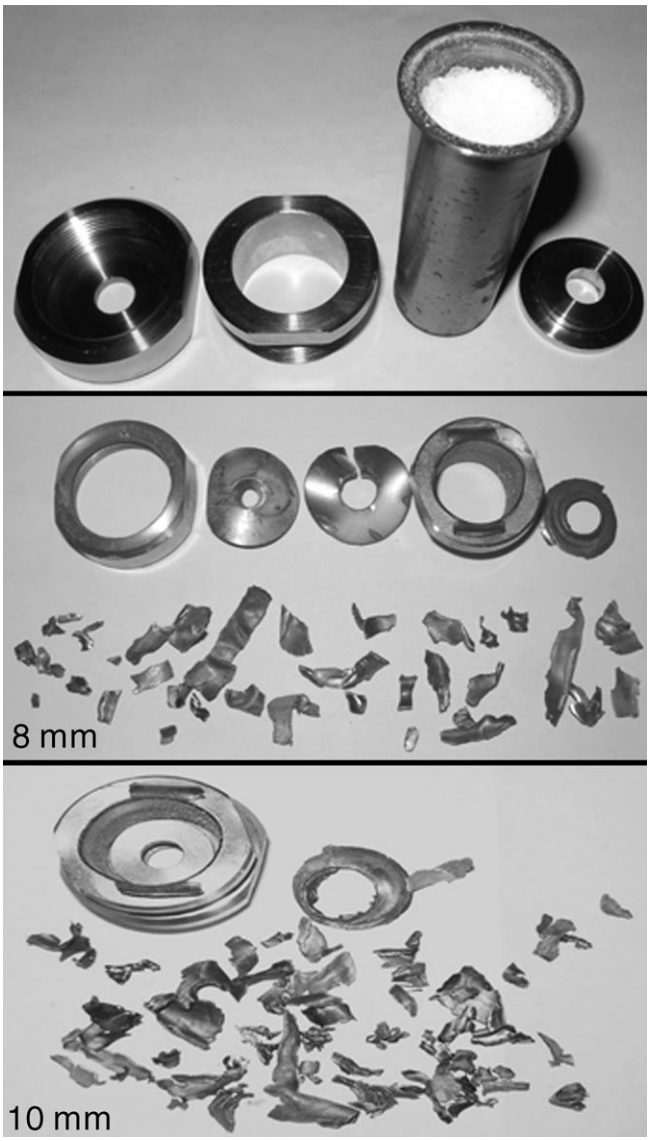

Fig. 11. Top: *Steel sleeve loaded with 25 ml* (30 g) *of compound* **5**. Middle: *Collected fragments using a hole width of 8 mm.* Bottom: *Collected fragments using a hole width of 10 mm.*

or endothermic behavior over a period of 48 h (*Fig. 12*). Compounds **2** and **5** were completely stable for 48 h, while **6** showed negligible minimal exothermic steps in the first 6 h. It can, therefore, be reasoned that all three compounds show long-term stability, which is a basic requirement for possible applications.

2.4.8. *Electrostatic Potential.* The electrostatic potentials were illustrated after computing an optimal geometry at the B3LYP/6-31G(d,p) level of theory using the

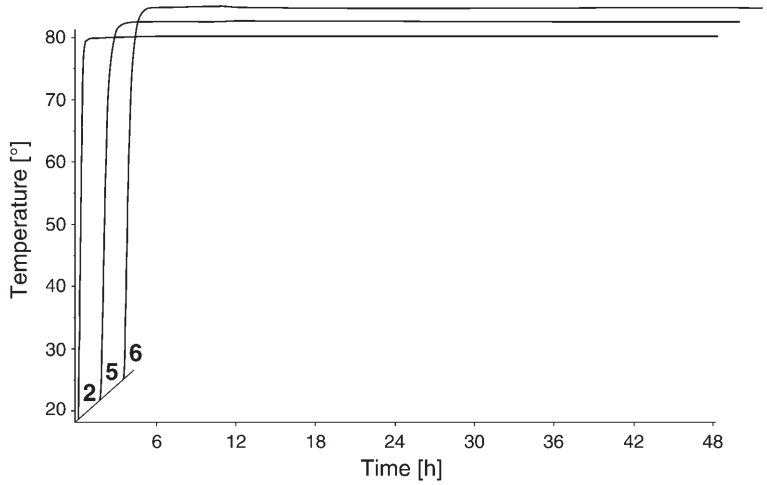

Fig. 12. *Long-term stability screen of* **2**, **5**, *and* **6** *using a FlexyTSC* (80°, 48 h)

program package HyperChem 7.52 [45]. *Fig. 13* shows the 0.001 electron/bohr^3 3D isosurface of electron density for **2**, **5**, and **6**. In these diagrams, a *Jorgensen–Salem* representation was chosen with an electrostatic potential contour value of 0.1 Hartree. The dark regions represent extremely electron-rich regions ($V(r) < 0.1$ Hartree and the light regions extremely electron-deficient regions ($V(r) > 0.1$ Hartree. In general, the patterns of the calculated electrostatic potentials of the surface of molecules can be related to the impact sensitivities [46][47]. In contrary to non-energetic organic molecules where the positive potential is larger but weaker in strength, in nitro and azo compounds usually more extensive regions with larger and stronger positive potentials are observed, which can be related to the increased impact sensitivities.

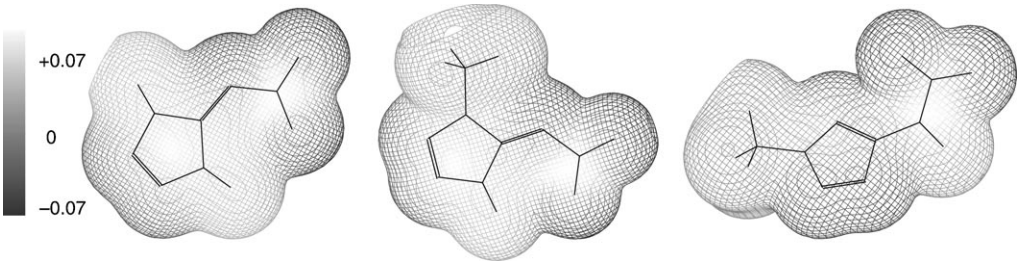

Fig. 13. *Calculated* (B3LYP/DFT/6-31G*(p,d)) *electrostatic potential of* **2** (*left*), **5** (*middle*), *and* **6** (*right*). The dark regions represent electron-rich regions, the light regions extremely electron-deficient regions.

3. Conclusions. – From this experimental study the following conclusions can be drawn:

- 5-(Nitrimino)-1*H*-tetrazole (**2**), 1-methyl-5-(nitrimino)-1*H*-tetrazole (**5**), and 2-methyl-5-(nitramino)-2*H*-tetrazole (**6**) can be synthesized in high yields and purity

from 5-amino-1*H*-tetrazole and 1- and 2-methyl-5-amino-1*H*- and -2*H*-tetrazole, respectively, in simple one-step syntheses by reaction with fuming HNO_3.

- The crystal structures of **2**, **5**, and **6** were determined by low-temperature single crystal X-ray diffraction. In the structure of **2**, both H-atoms could be located at the tetrazole ring forming a (nitrimino)tetrazole. A similar structure can be observed for **5**, whereas **6** corresponds to a (nitramino)tetrazole, where the H-atom is located at the N-atom of the nitramino group. All these compounds are stabilized in the crystalline state by strong intermolecular H-bonds.
- Thorough characterization of the chemical, thermochemical, and energetic properties of **2**, **5**, and **6** is reported. All compounds presented are promising energetic materials, showing increased sensitivities towards friction and impact. In the case of **2**, increased precautions should be undertaken when the compound is prepared on a larger scale.

Experimental Part

General. All reagents and solvents were used as received (*Sigma-Aldrich*, *Fluka*, *Acros Organics*) if not stated otherwise. 5-Amino-1*H*-tetrazole (97%) was purchased from *Aldrich*, HNO_3 (100%) from *Fluka*, and MeI from *Acros Organics*. M.p.: *Perkin-Elmer Pyris6 DSC* with heating rates of 5°/min or *Büchi Melting Point B-450* apparatus; not corrected. IR Spectra: *Perkin-Elmer Spektrum One* FT-IR instrument; KBr pellets; $\tilde{\nu}$ in cm^{-1}. *Raman* spectra: *Perkin-Elmer Spektrum 2000R* NIR FT-*Raman* instrument equipped with a Nd:YAG laser (1064 nm); $\tilde{\nu}$ in cm^{-1}. ^1H-, ^{13}C-, ^{14}N-, and ^{15}N-NMR spectra: *Jeol Eclipse-270*, *EX-400*, or *Eclipse-400* instrument, in (D_6)DMSO at 25°; chemical shifts δ in ppm rel. to TMS (^1H, ^{13}C) or $MeNO_2$ (^{14}N, ^{15}N); *J* in Hz. MS: *Jeol MStation JMS-700*; in *m*/*z* (rel.). Elemental analyses: *Netsch STA 429 Simultaneous Thermal Analyzer*. Bomb-calorimetry measurements: *Parr 1356* bomb calorimeter with a *Parr 1108CL* oxygen bomb. The sensitivity data were obtained using BAM methods.

CAUTION! *The (nitrimino)- and (nitramino)tetrazoles prepared are energetic materials which show increased sensitivities towards various stimuli. Proper protective measures (safety glasses, face shield, leather coat, earthened equipment and shoes,* Kevlar® *gloves and ear plugs) should be used when handling compound* **2**, **5**, *and* **6**. *Extra safety precautions should be taken, especially when compound* **2** *is prepared on larger scale.*

*4,5-Dihydro-5-(nitrimino)-1*H*-tetrazole* (**2**). *5-Amino-1*H*-tetrazole* (**1**; 4.25 g, 0.05 mol) was added in small portions to 15 ml of ice-cooled HNO_3 (100 %). After 2 h, the ice-bath was removed, and the soln. was stirred for further 20 h in an open vessel. (A closed reaction vessel favors the formation of the highly explosive *N*,*N*-dinitraminotetrazole!) The reaction was then quenched with 15 ml of cold water, and the HNO_3 was reduced in volume under vacuum until the colorless product started to precipitate. Single crystals suitable for X-ray diffraction were obtained by recrystallization of the crude product from half-conc. HNO_3. Yield: 5.98 g (92%) of **2**. M.p. 122° (dec.). IR: 3214*m*, 3081*m*, 2936*m*, 2857*m*, 1798*m*, 2720–2685*m* (br.), 2093*w*, 1708*w*, 1613*s*, 1507*s*, 1450*m*, 1405*m*, 1383*m*, 1515v*s*, 1236*s*, 1226*s*, 1130*w*, 1054*m*, 1021*m*, 995*m*, 878*m*, 780*m*, 752*m*, 714*m*, 653*m*, 478*w*, 399*m*. *Raman* (1064 nm): 3210 (2), 2707 (3), 1617 (98), 1599 (60), 1561 (15), 1523 (32), 1450 (70), 1407 (38), 1391 (30), 1309 (22), 1228 (68), 1120 (12), 1089 (47), 1054 (29), 1016 (68), 993 (61), 879 (17), 755 (100), 717 (16), 480 (70), 405 (29), 398 (28), 231 (40), 167 (29), 124 (19). ^1H-NMR: 14.21 (br., 2 H). ^{13}C-NMR: 152.6 (C(1)). ^{14}N-NMR: −24.6 (NO_2). ^{15}N-NMR: −24.6 (N(2), N(3), NO_2), −144.6 (N(1), N(4)), −174.9 (N(5)). DCI-MS: 131 ($[M+H]^+$), 85 ($[M+H-NO_2]^+$), 71 ($[CH_2N_4+H]^+$), 69 ($[M+H-H_2N_2O_2]^+$). DEI-MS: 130 (M^+), 84 ($[M-NO_2]^+$), 46 (NO_2^+), 42 (N_3^+), 28 (N_2^+). Anal. calc. for $CH_2N_6O_2$ (130.09): C 9.2, H 1.6, N 64.6; found: C 9.3, H 1.7, N 64.4. BAM-Drophammer: < 1.5 J. BAM-Friction Test: < 8.0 N. ΔU_c: 1700 cal/g.

*5-Amino-1-methyl-1*H*-tetrazole* (**3**) *and 5-Amino-2-methyl-2*H*-tetrazole* (**4**). The methylated aminotetrazoles were synthesized by methylation of 5-amino-1*H*-tetrazole using Me_2SO_4 or MeI according to the literature procedures [48]. An alternative synthesis proceeds *via* cyclization reactions according to the literature [49].

*4,5-Dihydro-1-methyl-5-(nitrimino)-1*H-*tetrazole* (**5**). Compound **3** (1.98 g, 0.02 mol) was added in small portions to 10 ml of ice-cooled HNO_3 (100 %). After 2 h, the ice-bath was removed, and the soln. was stirred for further 20 h. Afterwards, the reaction was quenched with 10 ml of cold water, and the HNO_3 was removed using high vacuum until the colorless product started to precipitate. Single crystals suitable for X-ray structure determination were obtained by recrystallization from half-conc. HNO_3. Yield: 2.74 g (95%) of **5**. M.p. 125° (dec.). IR: 3091–3056*m* (br.), 2885*m*, 2636*m*, 2282*w*, 2217*w*, 2082*w*, 1925*w*, 1591v*s*, 1515*s*, 1496*s*, 1455*s*, 1441*m*, 1411*m*, 1400*m*, 1384*m*, 1330v*s*, 1308*s*, 1261*s*, 1213v*s*, 1135*m*, 1065*w*, 1037*s*, 970*s*, 813*m*, 778*m*, 716*s*, 685*m*, 669*m*, 450*m*. *Raman* (1064 nm): 3057 (8), 3031 (9), 2966 (35), 1597 (58), 1574 (73), 1467 (24), 1441 (13), 1407 (100), 1310 (10), 1241 (59) 1218 (31), 1038 (61), 972 (38), 890 (23), 874 (15), 757 (44), 686 (57), 490 (32), 450 (14) 354 (10), 302 (42), 244 (19), 208 (19), 129 (10). ^{1}H-NMR: 14.09 (*s*, NH); 3.73 (*s*, Me). ^{13}C-NMR: 150.3 (C(1)); 34.0 (C(2)). ^{14}N-NMR: −18.8 (NO_2). ^{15}N-NMR: −26.8 (^3J(N,H) = 1.9, N(2)); −29.8 (N(3)); −159.2 (N(4)); −159.3 (N(5)); −177.4 (^2J(N,H) = 2.1, N(1)). DEI-MS: 144 (M^+), 46 (NO_2^+), 43 (HN_3^+), 15 (CH_3^+). Anal. calc. for $C_2H_4N_6O_2$ (144.11): C 16.7, H 2.8, N 58.3; found: C 16.6, H 2.8, N 58.5. BAM-Drophammer: < 12.5 J. BAM-Friction Test: < 160 N. ΔU_c: 2700 cal/g.

*2-Methyl-5-(nitramino)-2*H-*tetrazole* (**6**). Compound **4** (1.98 g, 0.02 mol) was added in small portions to 8 ml of ice-cooled HNO_3 (100 %). After 2 h, the ice-bath was removed, and the soln. was stirred at r.t. over night. The reaction was then quenched with 10 ml of ice, while the product precipitated. The colorless powder obtained was then recrystallized from hot water. Yield: 2.62 g (91%) of **6**. M.p. 123° (dec.). IR: 3237*m*, 3144*m*, 3051*s*, 2927*m*, 2819*m*, 2691*w*, 2402*w*, 1613v*s*, 1526*m*, 1479*s*, 1462*m*, 1384*m*, 1351*s*, 1313v*s*, 1207*m*, 1102*w*, 1051*w*, 1041*w*, 1001*w*, 920*m*, 779*m*, 759*m*, 734*m*, 691*m*, 618*w*, 482*w*. *Raman* (1064 nm): 3133 (9), 3052 (30), 2970 (98), 2828 (6), 1618 (10), 1524 (100), 1483 (35), 1438 (18), 1395 (24), 1359 (44), 1312 (43), 1209 (41), 1105 (40), 1042 (47), 1004 (50), 915 (16), 779 (13), 725 (6), 692 (72), 472 (17), 445 (61), 384 (47), 318 (29), 241 (15), 147 (20), 126 (18). ^{1}H-NMR: 11.74 (br. *s*, NH); 4.37 (*s*, Me). ^{13}C-NMR: 157.6 (C(1)); 40.9 (C(2)). ^{14}N-NMR: −35.0 (NO_2). ^{15}N-NMR: −0.3 (^3J(N,H) = 1.9, N(3)); −35.0 (NO_2); −58.3 (N(4)); −83.4 (N(1)); −103.6 (^2J(N,H) = 2.2, N(2)); −209.3 (N(5)); −159.2 (N(4)); −159.3 (N(5)); −177.4 (^3J(N,H) = 1.9, N(1)). DEI-MS: 144 (51, M^+), 98 (77, $[M - NO_2]^+$), 71 (9, $CH_3N_4^+$), 70 (15, $CH_2N_4^+$), 69 (10, CHN_4^+), 56 (27, N_4^+), 55 (30, CHN_3^+), 46 (21, NO_2^+), 43 (100, HN_3^+), 28 (43, N_2^+), 15 (33, CH_3^+). DCI-MS: 289 ($[2M + H]^+$), 145 ($[M + H]^+$), 99 ($[M - NO_2]^+$), 85 ($CH_3N_5^+$), 71 ($CH_3N_4^+$). Anal. calc. for $C_2H_4N_6O_2$ (144.11): C 16.7, H 2.8, N 58.3; found: C 16.8, H 2.9, N 58.4. BAM-Drophammer: < 3.0 J. BAM-Friction Test: < 145 N. ΔU_c: 2902 cal/g.

Crystallographic data for the structures **2**, **5**, and **6** reported in this article have been deposited with the *Cambridge CrystallographicData Centre* (*CCDC*). Copies of the data can be obtained free of charge on quoting the numbers 635164, 635163, and 635160 for **2**, **5**, and **6**, resp., from *CCDC* (12 Union Road, Cambridge, CB2 1EZ, UK (fax (internat.) +44(0)1223/336033; e-mail: deposit@ccdc.cam.ac.uk).

Financial support of this work by the University of Munich (LMU), the *Fonds der Chemischen Industrie*, the *European Research Office* (*ERO*) of the *U.S. Army Research Laboratory* (*ARL*) under contract no. N 62558-05-C-0027 & 9939-AN-01 and the *Bundeswehr Research Institute for Materials, Explosives, Fuels and Lubricants* (*WIWEB*) under contract no. E/E210/4D004/X5143 is gratefully acknowledged. The authors also thank Dr. *M.-J. Crawford* for correcting the manuscript, and *Gunnar Spiess* for the bomb-calorimetry measurements.

REFERENCES

[1] D. Adam, K. Karaghiosoff, G. Holl, M. Kaiser, T. M. Klapötke, *Propellants, Explosives, Pyrotechnics* **2002**, *27*, 7.
[2] K. Karaghiosoff, T. M. Klapötke, A. Michailovski, H. Nöth, M. Suter, *Propellants, Explosives, Pyrotechnics* **2003**, *28*, 1.
[3] T. M. Klapötke, P. Mayer, V. Verma, *Propellants, Explosives, Pyrotechnics* **2006**, *31*, 263.
[4] W. E. Deal, *J. Chem. Phys.* **1957**, *27*, 796.
[5] C. L. Mader, 'Report LA-2900: Fortran BKW Code for computing the detonation properties of explosives', Los Alamos Scientific Laboratory, Los Alamos, NM, July, 1963.

[6] T. Urbanski, 'Chemistry and technology of explosives', Pergamon Press, England, 1985.
[7] A. M. Astakhov, A. D. Vasilev, M. S. Molokeev, V. A. Revenko, R. S. Stepanov, *Russ. J. Org. Chem.* **2005**, *41*, 910.
[8] J. H. Bryden, *Acta Crystallogr.* **1953**, *6*, 669.
[9] K. Karahiosoff, T. M. Klapötke, P. Mayer, H. Piotrowski, K. Polborn, R. L. Willer, J. J. Weigand, *J. Org. Chem.* **2005**, *71*, 1295.
[10] B. C. Tappan, R. W. Beal, T. B. Brill, *Thermochim. Acta* **2002**, *288*, 227.
[11] B. C. Tappan, C. D. Incarnito, A. L. Rheingold, T. B. Brill, *Thermochim. Acta* **2002**, *384*, 113.
[12] T. B. Brill, B. C. Tappan, R. W. Beal, 'New Trends in Research of Energetic Materials. Proceedings of the 4th Seminar', Pardubice, 2001, p. 17.
[13] J. Thiele, *Liebigs Ann. Chem.* **1892**, *270*, 1.
[14] T. M. Klapötke, G. Kramer, G. Spieß, J. M. Welch, M. v. Denffer, G. Heeb, '8th Symposium on: New Trends in Research of Energetic Materials', Pardubice , April 19 – 21, 2005.
[15] R. M. Herbst, J. A. Garrison, *J. Org. Chem.* **1953**, *18*, 941.
[16] A. M. Astachov, A. A. Nefedo, A. D. Vasiliev, L. A. Kruglyakova, K. P. Dyugaev, R. S. Stepanov, '36th International Conference of ICT', Karlsruhe, June 28 – July 1, 2005, 113/1.
[17] E. Lieber, E. Sherman, R. A. Henry, J. Cohen, *J. Am. Chem. Soc.* **1951**, *73*, 2327.
[18] A. G. Mayants, V. S. Klimenko, V. V. Erina, K. G. Pyreseva, S. S. Gordeichuk, V. N. Leibzon, V. S. Kuz'min, U. N. Burtsev, *Khim. Geterot. Soed.* **1991**, *8*, 1067; M. Göbel, T. M. Klapötke, E. Mayer, *Z. Anorg. Allg. Chem.* **2006**, *632*, 1043.
[19] CrysAlis CCD, *Oxford Diffraction Ltd.*, Version 1.171.27p5 beta (release 01-04-2005 CrysAlis171.-NET; compiled April 1, 2005, 17:53:34).
[20] CrysAlis RED, *Oxford Diffraction Ltd.*, Version 1.171.27p5 beta (release 01-04-2005 CrysAlis171.-NET; compiled April 1, 2005, 17:53:34).
[21] A. Altomare, G. Cascarano, C. Giacovazzo, A. Guagliardi, 'SIR-92, A program for crystal structure solution', *J. Appl. Crystallogr.* **1993**, *26*, 343.
[22] G. M. Sheldrick, SHELXL97, Program for the Refinement of Crystal Structures, University of Göttingen, Göttingen, 1997.
[23] A. L. Spek, PLATON, A Multipurpose Crystallographic Tool, Utrecht University, Utrecht, 1999.
[24] SCALE3 ABSPACK, An Oxford Diffraction program (1.0.4,gui:1.0.3), *Oxford Diffraction Ltd.*, 2005.
[25] E. Lieber, S. Patinkin, H. H. Tao, *J. Am. Chem. Soc.* **1951**, *73*, 1792.
[26] D. D. Bray, J. G. White, *Acta Crystallogr., Sect. B* **1979**, *35*, 3089.
[27] E. Riedel, 'Anorganische Chemie', 4th edn., de Gruyter, Berlin, 1999, p. 134.
[28] E. Lieber, D. R. Levering, L. J. Patterson, *Anal. Chem.* **1951**, *23*, 1594.
[29] J. J. Weigand, Dissertation, Ludwig Maximilian University, Munich, 2005.
[30] Z. Daszkiewicz, E. M. Nowakowska, W. W. Preźdo, J. B. Kyzioł, *Pol. J. Chem.* **1995**, *69*, 1437.
[31] http://www.perkinelmer.com.
[32] http://www.linseis.com.
[33] http://www.parrinst.com.
[34] 'Handbook of Chemistry and Physics', 48th edn., Eds. R. C. West, S. M. Selby, The Chemical Rubber Co., Cleveland, 1967, pp. D22 – D51.
[35] V. A. Ostrovskii, M. S. Pevzner, T. P. Kofman, I. V. Tselinskii, *Targets Heterocycl. Syst.* **1999**, *3*, 467.
[36] 'UN Recommendations on the Transport of Dangerous Goods, Manual of Tests and Criteria', fourth revised edition, United Nations Publication, New York, Geneva, 2003, Sales No. E.03.VIII.2. Publication date: 13 January 2004.
[37] http://www.bam.de.
[38] A. M. Astakhov, R. S. Stepanov, L. A. Kruglyakova, A. A. Nefedov, *Russ. J. Org. Chem.* **2001**, *37*, 577.
[39] R. Mecke, F. Langenbucher, 'Infrared Spectra', Heyden & Son, London, 1965, Serial No. 6.
[40] T. Shimanouchi, *J. Phys. Chem. Ref. Data* **1972**, *6*, 993.
[41] http://webbook.nist.gov/chemistry/vib-ser.html.

[42] K. Nakamoto, 'Infrared and Raman Spectra of Inorganic and Coordination Compounds', 4th edn., John Wiley & Sons, New York, Chichester, Brisbane, Toronto, Singapore, 1986.
[43] EXPLO5.V2, software for determining detonation parameter, 2006.
[44] http://www.systag.ch.
[45] HyperChem 7.52, Molecular Visualization and Simulation Program Package, *Hypercube Inc.*, Gainsville, 2002.
[46] B. M. Rice, J. J. Hare, *J. Phys. Chem., A* **2002**, *106*, 1770.
[47] P. Politzer, J. S. Murray, J. M. Seminario, P. Lane, M. E. Grice, M. C. Concha, *J. Mol. Struct.* **2001**, *573*, 1; J. S. Murray, P. Lane, P. Politzer, *Mol. Phys.* **1995**, *85*, 1.
[48] R. A. Henry, W. G. Finnegan, *J. Am. Chem. Soc.* **1954**, *76*, 923.
[49] R. M. Herbst, C. W. Roberts, E. J. Harvill, *J. Org. Chem.* **1951**, *16*, 139.

Received July 23, 2007